Magnetic and transport characteristics in $Gd_{0.925}La_{0.075}Mn_2Ge_2$ with two-dimensional alignment of Mn atoms

T. Fujiwara and H. Fujii
Faculty of Integrated Arts & Sciences, Hiroshima University, Higashi-Hiroshima 739-8521, Japan

T. Shigeoka
Faculty of Science, Yamaguchi University, Yamaguchi 753-8512, Japan

(Received 28 July 2000; revised manuscript received 4 December 2000; published 16 April 2001)

We present our recent experimental results on magnetic and transport properties in intermetallic compound $Gd_{0.925}La_{0.075}Mn_2Ge_2$ with the $ThCr_2Si_2$-type layered structure. The results obtained indicate that $Gd_{0.925}La_{0.075}Mn_2Ge_2$ reveals two kinds of first order transitions below the ferrimagnetic Curie temperature T_{t1}, from canted ferrimagnetic to noncollinear antiferromagnetic states and from noncollinear antiferromagnetic to reentrant canted ferrimagnetic states at T_{t2} and T_{t3} with decreasing temperature. Between T_{t2} and T_{t3}, a field induced metamagnetism from noncollinear antiferromagnetism to canted ferrimagnetism appears at relatively lower fields, accompanied with fractal-like multistep transitions, the so called ''devil's stair case.'' Furthermore, a negative giant magnetoresistance effect ($\Delta\rho/\rho \sim 15\%$) is also observed at the field induced metamagnetic transition. The mechanism of this negative GMR is discussed on the basis of the results of comprehensive measurements of the resistivities using single-crystalline $Gd_{0.925}La_{0.075}Mn_2Ge_2$ and $TbMn_2Ge_2$. These unusual features might be characteristic of layered structure, two-dimensional alignment of Mn atoms.

DOI: 10.1103/PhysRevB.63.174440 PACS number(s): 75.30.Kz, 75.50.Ee, 75.70.Pa

I. INTRODUCTION

Among a lot of research on magnetism in intermetallic compounds containing manganese Mn and rare earth metals R, much attention has been paid to the system RMn_2Ge_2, because it revealed some unusual behavior, such as appearances of metamagnetic transition from noncollinear antiferromagnetism to canted ferromagnetism,[1–3] reentrant canted ferromagnetism,[4–6] and giant magnetoresistance[7–11] accompanied by the metamagnetic transition. The RMn_2Ge_2 compounds crystallize in the layered structure of $ThCr_2Si_2$-type body-centered tetragonal belonging to the space group $I4/mmm$ in which the Mn atoms lie on every forth layer stacked along the c axis. In this structure, we notice that the Mn sublattice forms a simple tetragonal framework and the Mn-Mn interlayer distance along the c-axis $R^c_{\text{Mn-Mn}}$ is almost 5.5 to 5.6 Å, whereas the Mn-Mn intralayer distance in the c plane $R^a_{\text{Mn-Mn}}$ is nearly 2.8–2.9 Å, being only half of $R^c_{\text{Mn-Mn}}$. Accordingly, we can expect that some interesting features reflecting such a layered structure, in particular, two-dimensional arrangement (2D) of Mn atoms, appear in the magnetism.

Magnetic properties of RMn_2Ge_2 have been intensively investigated by Shigeoka[2] and Fujii *et al.*[4,13] and Szytula *et al.*,[12] so far. After the systematic studies on magnetism, Fujii *et al.* have proposed a critical distance model for adjacent Mn-Mn interlayer coupling.[4,13] Here, we call it the ITC model, which yields a qualitative understanding of the tendency of exchange coupling between adjacent Mn sublayers. According to this model, the Mn moments in the same Mn sublayer ferromagnetically couple to each other, and the adjacent Mn-Mn interlayer exchange interaction $J^c_{\text{Mn-Mn}}$ depends on the Mn-Mn intralayer distance $R^a_{\text{Mn-Mn}}$ rather than the Mn-Mn interlayer distance $R^c_{\text{Mn-Mn}}$. Then, a critical distance of $R^a_{\text{Mn-Mn}}$ is deduced to be ~ 2.85 Å; $J^c_{\text{Mn-Mn}}$ is antiferromagnetic for $R^a_{\text{Mn-Mn}} \leqslant 2.85$ Å, while $J^c_{\text{Mn-Mn}}$ becomes ferromagnetic for $R^a_{\text{Mn-Mn}} > 2.85$ Å. In these days, the great advance in the neutron diffraction techniques have brought some detailed information on magnetic structure of a family of RMn_2Ge_2, among which especially the light rare earth compounds have revealed complex magnetic structure characterized by canted Mn moment arrangements,[5,6,14–16] such as a canted ferromagnetic structure with both ferromagnetic and antiferromagnetic components in the directions parallel and perpendicular to the c axis, respectively, or a conical structure composed of both ferromagnetic and helical components with the propagation vector parallel to the easy direction. On the basis of the above experimental results, Venturini and Welter *et al.*[5,6,14–16] have reported that the Mn-Mn intralayer exchange coupling $J^a_{\text{Mn-Mn}}$, namely, the Mn moment arrangement in the basal c plane depends on the Mn-Mn intralayer distance $R^a_{\text{Mn-Mn}}$ as well. Therefore, there is a similar critical distance of $R^a_{\text{Mn-Mn}} \sim 2.84$ Å for intralayer Mn-Mn exchange coupling, above which the Mn moments in intralayer noncollinear ferromagnetically couple to each other, leading to the canting of the Mn moments, but below which the Mn moments collinear ferromagnetically couple to each other within the same Mn sublayer. Here, we call the critical distance model for the Mn-Mn intralayer coupling the IRC model.

Among the light rare earth compounds with unusual magnetism, great interest has been paid to $SmMn_2Ge_2$. In this system with $R^a_{\text{Mn-Mn}} \sim 2.86$ Å at room temperature, Fujii *et al.*[4] and Tomka *et al.*[17,18] have observed two kinds of the first order transitions from canted ferromagnetic to noncollinear antiferromagnetic states at T_{t2} below the ferromagnetic Curie temperature T_{t1} and from the noncollinear antiferromagnetic to reentrant canted ferromagnetic states at T_{t3}

with decreasing temperature. In addition, a giant magnetoresistance (GMR) has been observed accompanied by a field induced metamagnetic transition from the noncollinear antiferromagnetic to canted ferromagnetic states. However, the origin of GMR is still unknown at present.

In order to clarify the correlation between magnetic and transport properties of the Mn sublattice in the system $R\mathrm{Mn_2Ge_2}$ in detail, we drew the following research plan. The Mn moments in $\mathrm{GdMn_2Ge_2}$ with $R^a_{\text{Mn-Mn}} \sim 2.85$ Å at room temperature orders antiferromagnetically below $T_N = 365$ K and it undergoes a first order transition at $T_{t3} = 95$ K with decreasing temperature, where the antiferromagnetism changes into ferrimagnetism.[2,19,20] In addition, since Gd is in a S state ($\langle \mathbf{S} \rangle = \frac{7}{2}$, $\langle \mathbf{L} \rangle = 0$), the $4f$ electrons in Gd do not contribute to the magnetocrystalline anisotropy. On the other hand, $\mathrm{LaMn_2Ge_2}$ with $R^a_{\text{Mn-Mn}} \sim 2.97$ Å (Refs. 19 and 21) shows a conical ferromagnetic structure, which consists of a ferromagnetic component along the c axis and a helical one in the c plane.[5] Since we can easily control $R^a_{\text{Mn-Mn}}$ to have the critical distances for the ITC and IRC models by substituting La for Gd in $\mathrm{GdMn_2Ge_2}$, we can expect the appearance of interesting magnetic and transport properties reflecting the layered structure in the system $\mathrm{Gd_{1-x}La_xMn_2Ge_2}$ because the environment of Mn atoms is very similar to that in $\mathrm{SmMn_2Ge_2}$.

Recently, Sokolov *et al.*[22] and Guanghua *et al.*[23] have studied the magnetic properties of $\mathrm{Gd_{1-x}La_xMn_2Ge_2}$ under similar expectation. Quite recently, they also gave an explanation for appearance of the ferrimagnetic to antiferromagnetic transition with decreasing temperature by applying the Yafet-Kittel model.[24] However, they applied the collinear model in their analysis and neglected the noncollinear Mn moment components in this system. Independently, we have investigated the magnetic properties of $\mathrm{Gd_{1-x}La_xMn_2Ge_2}$ with the composition range of $0 \leqslant x \leqslant 0.2$,[25] which gave similar results to those reported by Sokolov *et al.*[22] In this work, we studied the magnetic and transport properties in $\mathrm{Gd_{0.925}La_{0.075}Mn_2Ge_2}$ to clarify the origin of unusual magnetism and GMR observed in the system $R\mathrm{Mn_2Ge_2}$. The preliminary results have already been reported in Ref. 26.

II. EXPERIMENTAL PROCEDURE

Polycrystalline $\mathrm{Gd_{0.925}La_{0.075}Mn_2Ge_2}$ was prepared by the following procedure. After the binary alloy $\mathrm{Gd_{0.925}La_{0.075}}$ was prepared by arc melting under an Ar atmosphere, the polycrystalline sample was prepared by melting the mixture of stoichiometric amount of $\mathrm{Gd_{0.925}La_{0.075}}$, Ge, and about 5–10% excess Mn than the stoichiometry, for several times, which was necessary to compensate the loss while melting. Subsequently, the sample was wrapped in Mo foil, sealed into evacuated quartz tube and annealed for 1 week at 1173 K to ensure homogeneity. As a result of the powder x-ray diffraction (Cu-K_α) examination, the sample was confirmed to be single phase with the tetragonal $\mathrm{ThCr_2Si_2}$-type structure.

Single-crystalline samples of $\mathrm{Gd_{0.925}La_{0.075}Mn_2Ge_2}$ and $\mathrm{TbMn_2Ge_2}$ were grown by a Bridgeman method. Their polycrystalline samples were set in degassed MgO crucible, the crucibles with the samples were sealed into quartz tube under Ar gas, where the Ar gas pressure was controlled to become ~1 atm at the highest temperature, and heated up in a Bridgeman furnace. The samples were melted at 1633–1643 K just above the melting temperatures for 6 h. After then, the temperature was lowered to 1073 K at a rate of ~8 K per minute, kept at this temperature for 40 h and finally cooled in furnance. The weights of single crystals obtained by this method were 0.5–0.8 g.

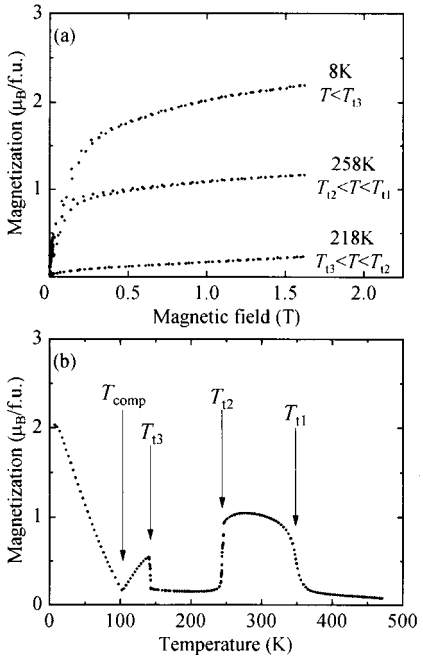

FIG. 1. Plots of (a) magnetization as a function of magnetic field at 8.0 K (below T_{t3}), 218 K (between T_{t3} and T_{t2}) and 258 K (between T_{t2} and T_{t1}) and (b) the magnetization at $H = 1.0$ T as a function of the temperature for $\mathrm{Gd_{0.925}La_{0.075}Mn_2Ge_2}$.

Measurements of the magnetization as a function of temperature between 4.2 and 480 K were performed on a vibrating sample magnetometer (VSM) in magnetic fields of 0.05 and 1 T. Measurements of the isothermal magnetization as a function of magnetic fields up to 1.6 T were performed using VSM in the field sweeping at a rate of 1.5 T per minute and the measuring temperatures were kept in an accuracy within ±0.05 K. The electrical resistivities as a function of temperature between 4.2 and 300 K were measured using a homemade equipment based on a standard four probe method under dc current of 50 mA. Magnetoresistance measurement was carried out using a superconducting magnet in the magnetic fields up to 6.0 T.

III. RESULTS AND DISCUSSION

A. Magnetic characteristics in $\mathrm{Gd_{0.925}La_{0.075}Mn_2Ge_2}$

Figures 1(a) and 1(b) show, respectively, the magnetization as a function of magnetic field at various temperatures and that at $H = 1.0$ T as a function of temperature for polycrystalline $\mathrm{Gd_{0.925}La_{0.075}Mn_2Ge_2}$. As is evident from Fig. 1, it behaves as ferrimagnets with the spontaneous magnetization at the temperatures of $T_{t2} < T = 258\,\mathrm{K} < T_{t1}$ and T

$=8\,\mathrm{K}<T_{t3}$, whereas no spontaneous magnetization is observed at the temperature $T_{t3}<T=218\,\mathrm{K}<T_{t2}$. These features indicate that $Gd_{0.925}La_{0.075}Mn_2Ge_2$ shows unusual multiple magnetic phase transitions in the sequence of paramagnetic, ferrimagnetic, antiferromagnetic and reentrant ferrimagnetic states accompanied with compensation phenomenon with decreasing temperature. We also notice that the polycrystalline $Gd_{0.925}La_{0.075}Mn_2Ge_2$ sample obtained in this work is quite good in quality, judging from the appearance of extremely sharp transitions at both $T_{t2}=244\,\mathrm{K}$ and $T_{t3}=142\,\mathrm{K}$.

According to the ITC model, the appearance of ferrimagnetism below T_{t1} originates in the positive $J^c_{\mathrm{Mn\text{-}Mn}}$, because $R^a_{\mathrm{Mn\text{-}Mn}}$ at room temperature is slightly larger than the critical distance 2.85 Å for the La composition of 0.075. With decreasing temperature, a first order transition from ferrimagnetism to antiferromagnetism occurs at T_{t2} because the shrinking of $R^a_{\mathrm{Mn\text{-}Mn}}$ is caused by thermal contraction and $R^a_{\mathrm{Mn\text{-}Mn}}$ becomes smaller than 2.85 Å at T_{t2}. Here, it should be noted that the Mn moments in the antiferromagnetic state as well as in the ferrimagnetic state order noncollinearly according to the IRC model. Because $R^a_{\mathrm{Mn\text{-}Mn}}$ is still larger than the critical distance 2.84 Å for the IRC model. With further decreasing temperature, it undergoes another first order transition at T_{t3}, where a canted reentrant ferrimagnetism appears due to enhancement of the antiferromagnetic exchange interaction between the Gd and Mn spins at lower temperature. Consequently, this indicates that the reentrantlike behavior as observed in $SmMn_2Ge_2$ is reproducible. Below T_{t3}, the compensation phenomenon that the Gd and Mn sublattice moments antiferromagnetically coupled to each other is also observable at T_{comp}.

At the lowest temperature, the Mn moment is supposed as $\sim 2.18\mu_B$ per Mn atom for $Gd_{0.925}La_{0.075}Mn_2Ge_2$ from the value of spontaneous magnetization if the Mn moments collinearly align in the intralayer and antiferromagnetically couple to the Gd moments. The deduced value is much smaller than that in $GdMn_2Ge_2$ even though the lattice constant increases by substituted La for Gd. This also suggests that the collinear Mn model is not applicable. Therefore, it seems that noncollinear ferrimagnetism is realized below T_{t3} for $Gd_{0.925}La_{0.075}Mn_2Ge_2$, in which the Mn moments cant from the *c* axis in the intralayer. The reentrant behavior obtained in this work is quite similar to that deduced by Guanghua *et al.*,[23] However, they claimed that the Mn moments in the intralayer were collinear-ferromagnetically ordered at any ordering temperatures in $Gd_{1-x}La_xMn_2Ge_2$ with the composition range of $0.05\leqslant x\leqslant 0.08$. On the other hand, we obtained somewhat different conclusion from their results; namely, the noncollinear Mn moment arrangement is stabilized for all the ordering temperature below T_{t1} in $Gd_{0.925}La_{0.075}Mn_2Ge_2$. In addition, we emphasize that the noncollinear Mn moment model is also acceptable from experimental results of magnetotransport measurements for $Gd_{0.925}La_{0.075}Mn_2Ge_2$, which will be described later.

On the basis of the above results, we can deduce magnetic structures in the temperature ranges of $T_{t2}\leqslant T\leqslant T_{t1}$, $T_{t3}\leqslant T\leqslant T_{t2}$, and $T\leqslant T_{t3}$ in $Gd_{0.925}La_{0.075}Mn_2Ge_2$, which are drawn in Figs. 2(a), 2(b), and 2(c), respectively. At $T\leqslant T_{t1}$, the intralayer arrangement of the Mn moments is noncollinear but ferromagnetic, in which the Mn moments cant from the *c* axis, but the Mn sublayer ferromagnetic components couple ferromagnetically to each other along the *c* axis. On the other hand, the Gd sublattice moments align ferromagnetically along the *c* axis by the exchange field from the Mn sublattice, and ferrimagnetically couple to the Mn moments [Fig. 2(a)]. With decreasing temperature, the system reveals unusual multiple magnetic phases, in which the Mn moments in the intralayer still maintains the same noncollinear and ferromagnetic ordering state, but the coupling tendency between the adjacent Mn sublayer canted ferromagnetic moments changes from ferromagnetic to antiferromagnetic as $R^a_{\mathrm{Mn\text{-}Mn}}\leqslant 2.85\,\text{Å}$ by lattice contraction. Consequently, three dimensional spin configuration with antiferromagnetic character is stabilized at $T_{t3}\leqslant T\leqslant T_{t2}$, where the molecular field from the Mn sublattice does not act on the Gd one, so that the Gd moments disorder [Fig. 2(b)]. However, the Gd-Mn exchange interaction becomes dominant at lower temperatures, the interaction of which is antiferromagnetic. Therefore, the Gd and Mn sublattice moments antiferromagnetically order at $T\leqslant T_{t3}$, since the Gd-Mn interlayer exchange interaction becomes sufficiently strong to overcome the Mn-Mn interlayer antiferromagnetic coupling, leading to reentrant canted ferrimagnetism as in Fig. 2(c).

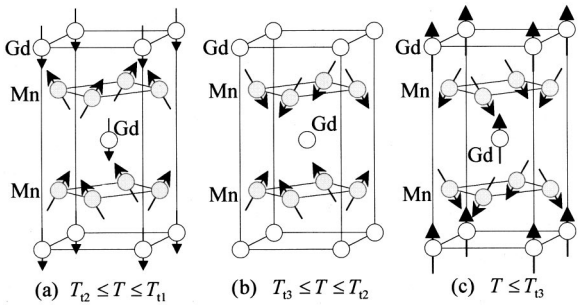

FIG. 2. Deduced magnetic structures at (a) $T_{t2}\leqslant T\leqslant T_{t1}$, (b) $T_{t3}\leqslant T\leqslant T_{t2}$, and (c) $T\leqslant T_{t3}$ for $Gd_{0.925}La_{0.075}Mn_2Ge_2$ on the basis of the critical distance ITC and IRC models.

Unfortunately it was impossible to determine the magnetic structures by neutron diffraction studies because of the very large absorption cross-section of the Gd atoms for thermal neutron. However, we believe that the deduced magnetic structure is acceptable from the fact that the ITC and IRC models are applicable without any exception in the system RMn_2Ge_2.

In Figs. 3(a) and 3(b), are shown the magnetizations in the noncolliner antiferromagnetic state as a function of magnetic field in some temperatures near both the first order transition temperatures T_{t2} and T_{t3} for $Gd_{0.925}La_{0.075}Mn_2Ge_2$ respectively. The $Gd_{0.925}La_{0.075}Mn_2Ge_2$ sample used in this work is a polycrystalline. Nevertheless, it is noticed that extremely sharp increases in magnetization appear at the first order metamagnetic transitions from noncollinear antiferromagnetism to canted ferrimagnetism. Most striking feature is that the magnetization process is accompanied by multistep in-

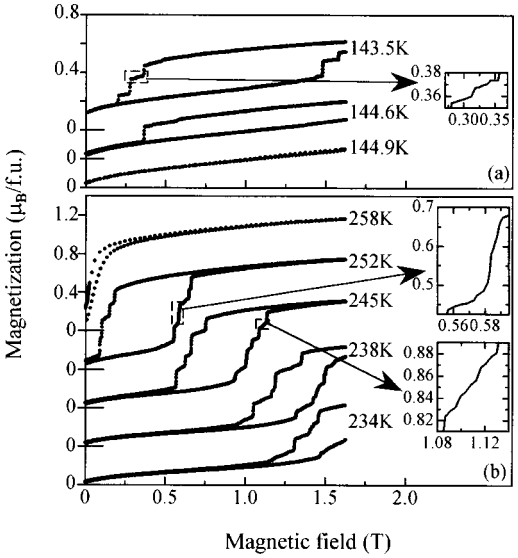

FIG. 3. Plots of magnetization as a function of magnetic field at various temperatures in the noncollinear antiferromagnetic state near the first order transition temperatures at T_{t2} and T_{t3} for $Gd_{0.925}La_{0.075}Mn_2Ge_2$.

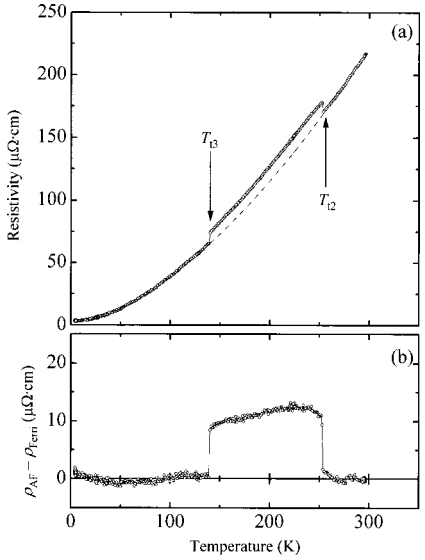

FIG. 4. Plots of (a) the resistivity as a function of temperature for polycrystalline $Gd_{0.925}La_{0.075}Mn_2Ge_2$ and broken line indicates the resistivity in the ferrimagnetic state obeying the $T^{1.6}$ law and (b) excess resistivity in the antiferromagnetic state compared with the ferrimagnetic state ($\rho_{AF}-\rho_{Ferri}$) in $Gd_{0.925}La_{0.075}Mn_2Ge_2$.

creases in magnetization, the so-called ''devil's stair case,'' which completely differs from that in the other RMn_2Ge_2 systems. Furthermore, when we expand an optional part of magnetization curve which looks similar to a straight line, we can clearly recognize that a lot of small discontinuous increase in magnetization occurs in the expanded flame. In addition, the fact that the feature in the expanded curve is similar to total feature in the original curve reminds us the word of ''fractals.'' As far as we know, such a fractal-like behavior has not been observed in any magnetization processes so far. Here, it should be noted that the results shown in Fig. 3 are those measured in a sweeping field rate of 1.5 T per minute. The magnetization curves measured in the sweeping rate of 0.15 T per minute also indicated the similar shapes to those in Fig. 3. Therefore, we believe that the fractal-like phenomenon observed in this work is substantial in the system $Gd_{0.925}La_{0.075}Mn_2Ge_2$.

The appearance of the fractals might be originated in the existence of the Mn atoms with different environments coming from statistical fluctuation of the La composition. That is, we consider that the spin-flip transition of the Mn moments may independently and locally occur in the noncollinear antiferromagnet at different magnetic fields in a microscopic scale, which leads to not only (1) a steplike formation of ferrimagnetic clusters, but also, (2) a steplike growth of their ferrimagnetic clusters with increasing magnetic field. As a consequence, the fractal-like multistep metamagnetism may appear. Such a state seems to be caused in the case that there are innumerable free energy minimum states in this spin system in the extremely narrow energy width, which occurs by statistical fluctuation of La composition. In addition, there is no doubt about that the behavior comes from the this spin system characterized by the following conditions: (1) being in a negligibly small magnetocrystalline anisotropy, (2) being in a competing state among several kinds of ferromagnetic and antiferromagnetic exchange interactions, and (3) being in an equivalent state, even if we see the spin structure along the any directions, i.e., having the three-dimensional degrees of freedom.

B. Transport characteristics in $Gd_{0.925}La_{0.075}Mn_2Ge_2$

Figure 4(a) shows the resistivity at $H=0$ as a function of temperature for the polycrystalline $Gd_{0.925}La_{0.075}Mn_2Ge_2$ sample. We can see two anomalies at 141 and 256 K, which clearly correspond to two kinds of first order transition temperatures T_{t2} and T_{t3} from canted ferrimagnetic to noncollinear antiferromagnetic and from the noncollinear antiferromagnetic to reentrant canted ferrimagnetic states, respectively. The result indicates that the resistivity in the antiferromagnetic state is about 10–15 % higher than that in the ferrimagnetic states. Except for the anomaly at $T_{t2}=256$ K, the ρ-T curve for $Gd_{0.925}La_{0.075}Mn_2Ge_2$ is quite similar to that for $GdMn_2Ge_2$.[2,20] It is of interest that the metallic behavior, the resistivity decreasing in proportion to $T^{\sim 1.6}$ with decreasing temperature, is observed over the magnetically ordered temperature regions. Here, the broken line indicates the resistivity in the hypothetic ferrimagnetic state obeying $T^{1.6}$ law, which was estimated in the customary fashion by plotting the logarithm of ferrimagnetic part by subtracted the residual resistivity from the observed resistivity $\ln[\rho_{Ferri}(T)-\rho(0)]$ against temperature T. The excess resistivity in the antiferromagnetic state compared with the ferrimagnetic state $\Delta\rho_{AF}=\rho_{AF}-\rho_{Ferri}$ is given in Fig. 4(b). The higher resistivity in the antiferromagnetic state than that in the ferrimagnetic state is in good agreement with the behavior of polycrystalline $SmMn_2Ge_2$ reported by Brabers *et al.*[8,9] Accordingly, it is expected that the giant magnetoresistance effect (GMR) at $T_{t3}<T<T_{t2}$ could be induced by the field

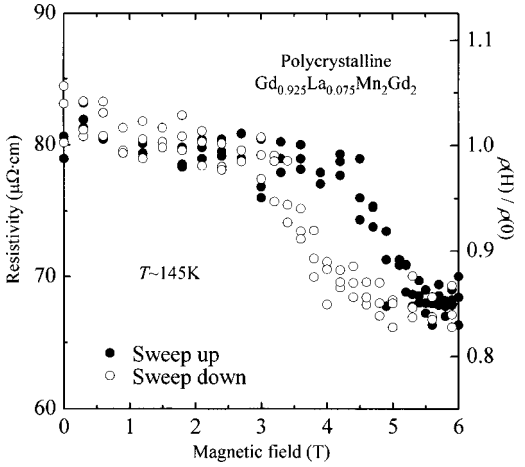

FIG. 5. Plots of the resistivity as a function of magnetic field at $T \sim 145$ K for polycrystalline $Gd_{0.925}La_{0.075}Mn_2Ge_2$.

induced metamagnetism from noncollinear antiferromagnetism to canted ferrimagnetism in $Gd_{0.925}La_{0.075}Mn_2Ge_2$ as well.

Figure 5 shows the resistivity as a function of magnetic field at ~145 K just above T_{t3}.[26] When the magnetic field is increased, an abrupt decrease of the resistivity appears at $H \sim 4.5$ T, while, on the decreasing field process, an abrupt increase is observed at $H \sim 3.7$ T. Because the resistivity was measured using short and thick specimen under high current, the accuracy of measurement is not so good and the measured points are scattered. However, it is to be noted that there is a possibility that the multi-step increase of magnetization affects to the scattering of the data points. Defining $[\rho(H)-\rho(0)]/\rho(0)$ as the magnetoresistance $\Delta\rho/\rho$, a negative giant magnetoresistance GMR of $\Delta\rho/\rho \cong -15\%$ is observed at $T \sim 145$ K accompanied by the metamagnetic transition from noncollinear antiferromagnetic to canted ferrimagnetic state. Recently, Sampathkumaran *et al.*[27] also observed the magnetoresistance $\Delta\rho/\rho \sim -6\%$ at the metamagnetic transition in $Gd_{0.93}La_{0.07}Mn_2Ge_2$, which is somewhat smaller than our data.

To clarify the origin of negative GMR, we carried out the measurements of magnetization and resistivity using single-crystalline $Gd_{0.925}La_{0.075}Mn_2Ge_2$ as well. The magnetization along the *c* axis (easy direction) at $H = 0.05$ T and the resistivities at $H = 0$ along the directions parallel and perpendicular to the *c* axis are shown in Fig. 6(a) as a function of temperature. In addition, the resistivities along both the directions in the ferrimagnetic state (broken lines) are drawn in Fig. 6(a), which were estimated by the same way as used for the polycrystalline. Compared to the result of polycrystalline sample, the temperature region where noncollinear antiferromagnetism is stabilized becomes narrow due to the broadening of the first order transitions corresponding to T_{t2} and T_{t3}. The cause of the broadening of both the transitions is because the composition fluctuation of consistent elements in the single-crystalline sample grown by the Bridgeman method is much larger than that in the polycrystalline sample prepared by arc melting, but not because of an intrinsic behavior of single-crystalline $Gd_{0.925}La_{0.075}Mn_2Ge_2$.

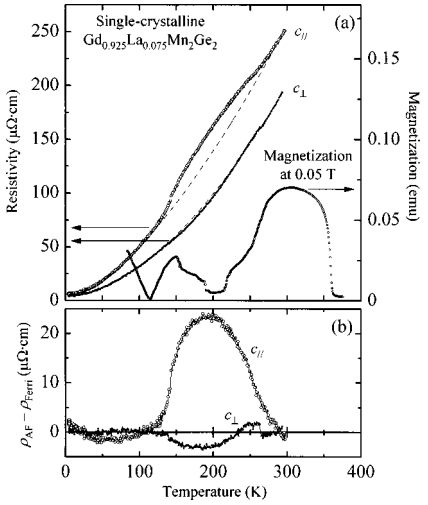

FIG. 6. Plots of (a) the magnetization at $H = 0.05$ T and resistivities along the *c* axis and *c* plane as a function of temperature for single-crystalline $Gd_{0.925}La_{0.075}Mn_2Ge_2$ and broken lines indicate the resistivities parallel and perpendicular to the *c* axis in the ferrimagnetic state obeying the $T^{1.5}$ and $T^{1.8}$ laws, respectively, and (b) excess resistivities along the *c* axis and *c* plane in the antiferromagnetic state compared with the ferrimagnetic state ($\rho_{AF}-\rho_{Ferri}$) in single-crystalline $Gd_{0.925}La_{0.075}Mn_2Ge_2$.

The overall temperature dependence of $\rho^{c\text{axis}}$ and $\rho^{c\text{plane}}$ is proportional to $T^{\sim 1.5}$ and $T^{\sim 1.8}$, respectively. The resistivity in the *c* plane is smaller than that along the *c* axis, suggesting that the Mn 3*d* electrons are more movable in the *c* plane than along the *c* axis, reflecting the 2D arrangement of Mn atoms. As is seen in Fig. 6(a), a hump appears in temperatures between $T_{t3} \sim 140$ K and $T_{t2} \sim 260$ K in the $\rho^{c\text{axis}}$-*T* curve. This obviously indicates that the antiferromagnetic ordering is accompanied by the increment of the resistivity along the *c* axis, which is similar to the behavior of polycrystalline sample. On the other hand, the $\rho^{c\text{plane}}$-*T* curve reveals that a small anomaly occurs at $T \sim 250$ K corresponding to the first order transition temperature T_{t2}, whereas no anomaly is observed near the temperature corresponding to $T_{t3} = 140$ K. The excess resistivities $\Delta\rho_{AF} = \rho_{AF} - \rho_{Ferri}$ along the directions parallel and perpendicular to the *c* axis are shown in Fig. 6(b). The excess contribution to the *c*-axis resistivity due to antiferromagnetic ordering $\Delta\rho_{AF}^{c\text{axis}}$ was evaluated to be $\sim 24\ \mu\Omega$ cm at $T \sim 200$ K, which is almost twice of the value for the polycrystalline. This implies that the results of overall resistivities for polycrystalline sample mainly reflect the transport properties along the *c* axis. It is inferred that the increase in the resistivity due to antiferromagnetic ordering originates in the reconstruction of the Fermi surface, which is accompanied with the appearance of antiferromagnetic ordering.

Here, we assume that the resistivity due to scattering from the Mn sublattice is essential and the Mn sublayer moments are directed parallel to the *c* axis and ferromagnetically couple to each other in the ferrimagnetic state. On the other hand, in the antiferromagnetic state, the adjacent Mn sublayer moments are assumed to be antiferromagnetically coupled to each other, i.e., the Mn sublayer moment aligns

with the sequence of $+ - + -$ along the c axis. Then, the magnetic superstructure is formed, where the magnetic c parameter is twice as large as the lattice constant c of the Mn sublattice. As a result of development of the antiferromagnetic ordering, the band gap along the c direction is formed within the first brillouin zone by a truncation of the Fermi surface, leading to an effective reduction in the numbers of conduction electrons and a dramatic increase in the resistivity along the c axis. Regardless of the intermetallic compounds, such a band structure effect frequently plays an important role in the transport properties in localized or itinerant spin systems. A layered uranium intermetallics UNiGa,[28,29] for example, is a typical material showing a negative GMR for the localized spin system, and in the Cr and Cr-Mn alloys[30] with CsCl-type crystal structure, a drastic enhancement in the resistivity is observed below Néel temperature T_N, which are known as an itinerant electron antiferromagnet.

In fact, the Mn moments in $Gd_{0.925}La_{0.075}Mn_2Ge_2$ do not follow such a collinear antiferromagnetic model, but couple noncollinear antiferromagnetically to each other. Therefore, the noncollinear and antiferromagnetic configuration in $Gd_{0.925}La_{0.075}Mn_2Ge_2$ complicatedly contributes to the c-plane resistivity, judging from the results in Fig. 6(b). The c-plane resistivity in the antiferromagnetic state is slightly larger than that in the ferrimagnetic state in temperatures between ~240 and ~260 K, while it obviously tends to become lower than the resistivity in the ferrimagnetic state in the temperature region of $140\,\mathrm{K} < T < 240\,\mathrm{K}$. These complicated features imply that some positive and negative contributions coexist in the c-plane resistivity. Van Dover *et al.*[7] have reported that the c-plane resistivity of single-crystalline $SmMn_2Ge_2$ becomes 4–8% lower in the antiferromagnetic state than that in the ferromagnetic state. Tomka *et al.*[17,18] gave a good account for the negative contribution to the c-plane resistivity due to the antiferromagnetic arrangement on the basis of magnetic structures of $SmMn_2Ge_2$ determined from their neutron diffraction studies. As is described above, the canted Mn moment configurations, namely, noncollinear magnetic structures, appear in all the ordering temperatures below $T_{t1} \sim 350\,\mathrm{K}$ for $Gd_{0.925}La_{0.075}Mn_2Ge_2$. They hypothesized that the antiferromagnetic component within the Mn intralayer should be functionable as a scattering factor of conduction electrons in the c plane. In the case of the system $SmMn_2Ge_2$, the antiferromagnetic component within the c plane in the antiferromagnetic state at $T_{t3} < T < T_{t2}$ and $H < H_C$ becomes smaller than that in any other magnetic ordered states with ferromagnetic components containing the field induced ferromagnetic state at $T_{t3} < T < T_{t2}$ and $H > H_C$. This results in $\rho_{\mathrm{AFl}}^{\mathrm{cplane}} < \rho_{\mathrm{F}}^{\mathrm{cplane}}$ irrespective of whether magnetic field is applied for the system. Thus, the origin of the anomalous behavior in the c-plane resistivity of $SmMn_2Ge_2$ could be understood in terms of the Mn spin-valve scattering mechanism.

The hypothesis of Tomka *et al.*[17,18] leads us to the conclusion that the canted Mn moment configurations are stabilized at all the magnetically ordered temperature below $T_{t1} = 348\,\mathrm{K}$ in $Gd_{0.925}La_{0.075}Mn_2Ge_2$ in analogy with $SmMn_2Ge_2$, and the antiferromagnetic structure in the c plane might play an important role in unusual behaviors such as the lower c-plane resistivity in the antiferromagnetic state than that in the ferrimagnetic state in $Gd_{0.925}La_{0.075}Mn_2Ge_2$.

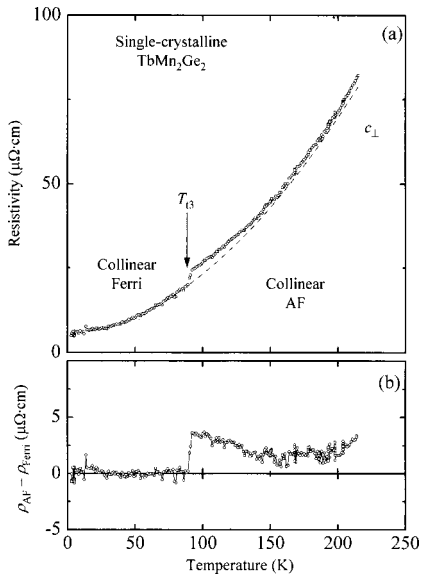

FIG. 7. Plots of (a) the resistivity and (b) excess resistivity ($\rho_{\mathrm{AF}}^{\mathrm{cplane}} - \rho_{\mathrm{Ferri}}^{\mathrm{cplane}}$) within the c plane as a function of temperature for single-crystalline $TbMn_2Ge_2$ and broken line indicates the resistivity within the c plane in the ferrimagnetic state obeying the $T^{1.8}$ law.

To clarify the origin of the unusual behavior, we further studied the c-plane resistivity measurement on single crystalline $TbMn_2Ge_2$ in this work. Morellon *et al.*[31] and Venturini *et al.*[32] have independently performed the neutron diffraction studies of $TbMn_2Ge_2$ and finally verified that $TbMn_2Ge_2$ orders the collinear antiferromagnetism below $T_N = 417\,\mathrm{K}$ and it undergoes a first order transition at $T_{t3} = 95\,\mathrm{K}$ with decreasing temperature, at which the magnetic structure transforms from collinear antiferromagnetic into collinear ferrimagnetic configurations. Therefore, it is of interest to know how the c-plane resistivity does behave, when the magnetic structure changes from collinear ferrimagnetic to antiferromagnetic states at T_{t3}. Figure 7(a) shows the c-plane resistivity as a function of temperature for a single-crystalline $TbMn_2Ge_2$. The overall temperature dependence is followed to the same $T^{-1.8}$ law as in $Gd_{0.925}La_{0.075}Mn_2Ge_2$. As is evident from this figure, an anomaly is seen at the first order transition temperature T_{t3}, indicating that the c-plane resistivity slightly increases by the appearance of collinear antiferromagnetic ordering along the c axis. The positive excess c-plane resistivity in the antiferromagnetic state is about 3–4 $\mu\Omega\,\mathrm{cm}$ coming from magnetic structure change along the c axis. Hence, it is deduced that the unusual behavior of the c-plane resistivity in $Gd_{0.925}La_{0.075}Mn_2Ge_2$ is attributed to the competition between the positive and negative contributions to the resistivity due to the antiferromagnetic orderings along the c axis and in the c plane, respectively, and different temperature dependence of the both contributions.

Finally, it is noteworthy that the appearances of both the temperature induced negative and positive magnetoresistance

effects in the *c*-plane resistivities in $Gd_{0.925}La_{0.075}Mn_2Ge_2$ and $TbMn_2Ge_2$ strongly supports that the noncollinear Mn moments configurations are stabilized at any magnetically ordered states below T_{t1} in $Gd_{0.925}La_{0.075}Mn_2Ge_2$. This gives a quite reasonable agreement with the conclusion we obtained according to the ITC and IRC models.

IV. CONCLUSION

We have studied the magnetic and transport properties of layered compound $Gd_{0.925}La_{0.075}Mn_2Ge_2$. The results obtained are summarized as follows.

(1) In $Gd_{0.925}La_{0.075}Mn_2Ge_2$, multiple magnetic phase transitions below the ferrimagnetic Curie temperature T_{t1} appear with decreasing temperature in the sequence of paramagnetic, canted ferrimagnetic, noncollinear antiferromagnetic, reentrant canted ferrimagnetic states. Consequently, the reentrantlike behavior is reproducible in this system similar to that reported in $SmMn_2Ge_2$. Here, it is deduced that all the magnetically ordered states observed in this work are characterized by three-dimensional noncollinear magnetic structures with the Mn moment components along the *c*-axis and in the *c*-plane.

(3) In the isothermal magnetization curves for polycrystalline $Gd_{0.925}La_{0.075}Mn_2Ge_2$, extremely sharp field induced metamagnetism appears near T_{t2} and T_{t3} where the phase transitions from canted ferrimagnetic to noncollinear antiferromagnetic states and from the antiferromagnetic to reentrant canted ferrimagnetic states occur. The most striking feature is that the metamagnetic transition is accompanied by a fractal-like multistep increase in magnetization, the so-called ''devil's stair case.'' We would like to emphasis that such a fractal-like phenomenon in magnetization curve was for the first time observed in this work.

(4) As a result of the resistivity measurement as a function of magnetic field at $T \sim 145\,K$ for polycrystalline $Gd_{0.925}La_{0.075}Mn_2Ge_2$, a negative giant magnetoresistance $(\Delta\rho/\rho \cong -15\%)$ is observed, which is accompanied with a metamagnetic transition.

(5) From the measurements of resistivities along the directions parallel and perpendicular to the *c* axis as a function of temperature for single-crystalline $Gd_{0.925}La_{0.075}Mn_2Ge_2$, it was deduced that the increment of 20–30 % occurs in the resistivity along the *c* axis at the magnetic phase transition from canted ferrimagnetic to noncollinear antiferromagnetic states.

(6) In addition, from the results of resistivity measurement in the *c* plane as a function of temperature for single-crystalline $TbMn_2Ge_2$, it was found that not only the temperature induced positive magnetoresistance effect due to the change of the *c*-axis moment component from ferrimagnetic to antiferromagnetic ordering, but also the temperature induced negative magnetoresistance effect in the *c* plane coexist in $Gd_{0.925}La_{0.075}Mn_2Ge_2$, but the former contribution is much larger than the latter one, which result in a negative GMR in polycrystalline $Gd_{0.925}La_{0.075}Mn_2Ge_2$.

ACKNOWLEDGMENTS

The authors thank Dr. H. Kobayashi at Tohoku University for his great useful advice on growth techniques of single crystals. We also thank Dr. H. Fukuda at Hiroshima University for some discussion and the cryogenic center at Hiroshima University for supplying a liquid helium and the use of a vibrating sample magnetometer to perform magnetization measurements.

[1] A. Szytula, in *Ferromagnetic Materials*, edited by K. H. J. Buschow (North-Holland, Amsterdam, 1991), Vol. 6, p. 85.
[2] T. Shigeoka, J. Sci. Hiroshima Univ., Ser. A: Phys. Chem. **48**, 103 (1985).
[3] T. Kaneko, T. Kanomata, H. Yasui, T. Shigeoka, N. Iwata, and Y. Nakagawa, J. Phys. Soc. Jpn. **61**, 4164 (1992).
[4] H. Fujii, T. Okamoto, T. Shigeoka, and N. Iwata, Solid State Commun. **53**, 715 (1985).
[5] G. Venturini, R. Welter, E. Ressouche, and B. Malaman, J. Alloys. Compnd. **210**, 213 (1994).
[6] R. Welter, G. Venturini, E. Ressouche, and B. Malaman, J. Alloys. Compnd. **218**, 204 (1995).
[7] R. B. van Dover, E. M. Gyorgy, R. J. Cava, J. J. Krajewski, R. J. Felder, and W. F. Peck, Phys. Rev. B **47**, 6134 (1993).
[8] J. H. V. J. Brabers, K. Bakker, H. Nakotte, F. R. de Boer, S. K. J. Lenczowski, and K. H. J. Buschow, J. Alloys. Compnd. **199**, L1 (1993).
[9] J. H. V. J. Brabers, A. J. Noten, F. Kayzel, S. H. J. Lenczowski, K. H. J. Buschow, and F. R. de Boer, Phys. Rev. B **50**, 16 410 (1994).
[10] E. V. Sampathkumaran, P. L. Paulose, and R. Malik, Phys. Rev. B **54**, R3710 (1996).
[11] R. Mallik, E. V. Sampathkumaran, and P. L. Paulose, Physica B **230–232**, 731 (1997).
[12] A. Szytula and S. Siek, J. Magn. Magn. Mater. **27**, 49 (1982).
[13] H. Fujii, M. Isoda, T. Okamoto, T. Shigeoka, and N. Iwata, J. Magn. Magn. Mater. **54–57**, 1345 (1986).
[14] G. Venturini, R. Welter, E. Ressouche, and B. Malaman, J. Magn. Magn. Mater. **150**, 197 (1995).
[15] G. Venturini, R. Welter, E. Ressouche, and B. Malaman, J. Alloys. Compnd. **223**, 101 (1995).
[16] G. Venturini, B. Malaman, and E. Ressouche, J. Alloys. Compnd. **241**, 135 (1996).
[17] G. J. Tomka, Cz. Kapusta, C. Ritter, P. C. Riedi, R. Cysinski, and K. H. J. Buschow, Physica B **230**, 727 (1997).
[18] G. J. Tomka, C. Ritter, P. C. Riedi, Cz. Kapusta, and W. Kocemba, Phys. Rev. B **58**, 6330 (1998).
[19] K. S. V. L. Narasimhan, V. U. S. Rao, R. L. Bergner, and W. E. Wallace, J. Appl. Phys. **46**, 4957 (1976).
[20] T. Shigeoka, H. Fujii, H. Fujiwara, K. Yagasaki, and T. Okamoto, J. Magn. Magn. Mater. **31–34**, 209 (1983).
[21] T. Shigeoka, N. Iwata, H. Fujii, and T. Okamoto, J. Magn. Magn. Mater. **53**, 83 (1985).

[22] A. Sokolov, H. Wada, M. Shiga, and T. Goto, Solid State Commun. **105**, 289 (1998).
[23] Guo Guanghua, R. Z. Levitin, A. Yu. Sokolov, V. V. Snegirev, and D. A. Flippov, J. Magn. Magn. Mater. **214**, 301 (2000).
[24] Y. Yafet and C. Kittel, Phys. Rev. **87**, 290 (1952).
[25] T. Fujiwara, H. Fujii, and T. Shigeoka, J. Magn. Soc. Jpn. **23**, 477 (1999).
[26] T. Fujiwara, H. Fujii and T. Shigeoka, Physica B **281&282**, 161 (2000).
[27] E. V. Sampathkumaran, S. Majumdar, R. Mallik, R. Vijayaraghavan, H. Wada, and M. Shiga, J. Phys.: Condens. Matter **12**, L399 (2000).
[28] V. Sechovsk'y, L. Havela, L. Jirman, W. Ye, T. Takabatake, H. Fujii, E. Bruck, F. R. de Boer, and H. Nakotte, J. Appl. Phys. **70**, 5794 (1991).
[29] V. N. Antonov, A. Ya, Perlov, P. M. Oppeneer, A. N. Yaresko, and S. V. Halilov, Phys. Rev. Lett. **77**, 5253 (1996).
[30] S. Maki and K. Adachi, J. Alloys. Compnd. **46**, 1131 (1979).
[31] L. Morellon, P. A. Algarabel, and M. R. Ibarra, Phys. Rev. B **55**, 12 363 (1997).
[32] G. Venturini, B. Malaman, and E. Ressouche, J. Alloys. Compnd. **240**, 139 (1996).